JOURNAL OF GEOPHYSICAL RESEARCH, VOL. 114, G00E04, doi:10.1029/2008JG000870, 2009

Improved estimates of forest vegetation structure and biomass with a LiDAR-optimized sampling design

Todd J. Hawbaker,[1] Nicholas S. Keuler,[2] Adrian A. Lesak,[1] Terje Gobakken,[3] Kirk Contrucci,[4] and Volker C. Radeloff[1]

Received 10 October 2008; revised 7 May 2009; accepted 11 June 2009; published 23 September 2009.

[1] LiDAR data are increasingly available from both airborne and spaceborne missions to map elevation and vegetation structure. Additionally, global coverage may soon become available with NASA's planned DESDynI sensor. However, substantial challenges remain to using the growing body of LiDAR data. First, the large volumes of data generated by LiDAR sensors require efficient processing methods. Second, efficient sampling methods are needed to collect the field data used to relate LiDAR data with vegetation structure. In this paper, we used low-density LiDAR data, summarized within pixels of a regular grid, to estimate forest structure and biomass across a 53,600 ha study area in northeastern Wisconsin. Additionally, we compared the predictive ability of models constructed from a random sample to a sample stratified using mean and standard deviation of LiDAR heights. Our models explained between 65 to 88% of the variability in DBH, basal area, tree height, and biomass. Prediction errors from models constructed using a random sample were up to 68% larger than those from the models built with a stratified sample. The stratified sample included a greater range of variability than the random sample. Thus, applying the random sample model to the entire population violated a tenet of regression analysis; namely, that models should not be used to extrapolate beyond the range of data from which they were constructed. Our results highlight that LiDAR data integrated with field data sampling designs can provide broad-scale assessments of vegetation structure and biomass, i.e., information crucial for carbon and biodiversity science.

Citation: Hawbaker, T. J., N. S. Keuler, A. A. Lesak, T. Gobakken, K. Contrucci, and V. C. Radeloff (2009), Improved estimates of forest vegetation structure and biomass with a LiDAR-optimized sampling design, *J. Geophys. Res.*, *114*, G00E04, doi:10.1029/2008JG000870.

1. Introduction

[2] Vegetation structure is of key importance when quantifying forest resources [*Maclean and Krabill*, 1986; *Nelson et al.*, 1988], the availability of wildlife habitat [*Bergen et al.*, 2007; *Hyde et al.*, 2006; *MacArthur and MacArthur*, 1969], and the functioning of ecosystem processes [*Cramer et al.*, 2001; *Gower et al.*, 1999]. Optical satellite data have been used to map and quantify vegetation type [*Bauer et al.*, 1994; *Wolter et al.*, 1995], structure [*Cohen and Spies*, 1992; *Jakubauskas and Price*, 1997], and forest biomass [*Fassnacht et al.*, 1997; *Gower et al.*, 1999; *Zheng et al.*, 2004]. However, optical satellite data do not provide direct measurements of vegetation structure attributes such as tree height. Thus, the conceptual models linking vegetation structure to optical data may vary among ecosystems and vegetation types.

[3] In contrast, light detection and ranging (LiDAR) sensors rely on reflected laser pulses to measure ground and vegetation heights directly, and that makes them ideal for mapping the structure of vegetation [*Næsset*, 1997b]. Additionally, LiDAR is well suited for quantifying forest biomass and timber volume because these forest attributes are directly related to the vertical distribution of LiDAR pulses [*Næsset*, 1997a; *Nelson et al.*, 1984, 1988; *Nilsson*, 1996]. Consequently, LiDAR data are being increasingly used for ecological studies [*Lefsky et al.*, 2002] and habitat modeling [*Goetz et al.*, 2007; *Vierling et al.*, 2008], but most study areas have been relatively small and broad-scale applications have been noticeably lacking (but see *Næsset et al.* [2004]).

[4] Quantifying vegetation structure and biomass across broad spatial extents has been limited in part by the lack of LiDAR data. Even when data are available, the sheer volume of information presents a significant computational barrier, especially when high-density pulses are collected (>1 pulse/m^2). However, high-density LiDAR

[1]Department of Forest and Wildlife Ecology, University of Wisconsin-Madison, Madison, Wisconsin, USA.
[2]Department of Statistics, University of Wisconsin-Madison, Madison, Wisconsin, USA.
[3]Department of Ecology and Natural Resource Management, Norwegian University of Life Sciences, Ås, Norway.
[4]Ayers Associates, Inc., Madison, Wisconsin, USA.

0148-0227/09/2008JG000870$09.00

data, while necessary for individual tree crown delineation [*Brandtberg et al.*, 2003; *Hyyppä et al.*, 2001; *Leckie et al.*, 2003], may not be required for more general characterization of vegetation structure and biomass. Low-density (<1 pulse/m^2) LiDAR data have been useful for quantifying vegetation structure and biomass [*Gobakken and Næsset*, 2008; *Magnusson et al.*, 2007]. Low-density LiDAR data are becoming increasingly available in the U.S. through the Federal Emergency Management Agency (FEMA) flood hazard mapping program (http://www.fema.gov/plan/prevent/fhm/lidar_4b.shtm) and other state and regional efforts to update digital elevation models. These data offer promise for mapping vegetation structure at regional scales (T. J. Hawbaker et al., LiDAR-based measures of mixed hardwood forest structure, submitted to *Forest Science*, 2009).

[5] Most LiDAR data are collected by airborne sensors, but there are also spaceborne LiDAR missions. Currently, the Ice, Cloud, and land Elevation Satellite (ICESAT) is collecting LiDAR data that can provide information on vegetation structure [*Harding and Carabajal*, 2005; *Lefsky et al.*, 2005a]. However, ICESAT was not originally designed to measure vegetation, and its large footprint limits its utility for this purpose. This is why NASA is currently planning a new mission (Deformation, Ecosystem Structure, and Dynamics of Ice (DESDynI), http://desdyni.jpl.nasa.gov/ [*Donnellan et al.*, 2008]), to collect data on vegetation structure across the globe. The mission concept for DESDynI envisions a combination of LiDAR sensors, which will collect data along transects, and InSAR sensors for wall-to-wall coverage. Both the increasing availability of airborne LiDAR data and the promise of spaceborne missions present exciting opportunities for broad-scale mapping of vegetation structure and biomass, which will provide crucial information for carbon and biodiversity science.

[6] The scientific challenges that remain though are twofold. The first is how to derive biological information from LiDAR data over large spatial extents efficiently, and the second is how to obtain the field data needed to correlate LiDAR data with tree height, basal area, biomass, etc. Neither of these challenges is trivial. In regards to the first challenge, *Næsset* [2002] pioneered methods to calculate indices of pulse density at different heights from single-return LiDAR data. The advantage of this approach is that it reduces the data volume considerably (all LiDAR returns within a given grid cell are summarized into 20 indices), and that it allows for efficient wall-to-wall mapping. Initial applications of this approach were largely limited to boreal forests with low tree species diversity, and dominated by conifers [*Næsset*, 2002, 2004], but the approach has also been successfully applied to temperate, deciduous forests (Hawbaker et al., submitted manuscript, 2009), and warrants further testing in other forest types.

[7] The efficient collection of field data is the second challenge limiting the broad-scale applications of LiDAR and other remotely sensed data for quantifying vegetation structure and biomass. Without field data, LiDAR provides only absolute data on the height of the pulse reflections, and all derived data on vegetation structure and biomass are relative to those heights. Field data are essential to relate with LiDAR height measurements for broad-scale assessments of vegetation structure. The challenge is that good field data are not easy to obtain. Vegetation is often highly variable in space and it is expensive and time consuming to collect enough field data to capture the full range of variability over broad spatial extents. Large areas need to be covered and traveling among sampling sites is time consuming in remote locations. Field plot sizes often need to be large to correspond to the pixel size of remotely sensed data, but large plots take time to measure, mainly because measurements of vegetation structure, such as tree height, are time-consuming [*Avery and Burkhart*, 2002]. Resources for ground truth data collection are often limited and as a result, the accuracy of vegetation structure and biomass estimates may be limited by small sample sizes. There may also be measurement errors in field data which propagate into broad-scale estimates [*Westfall*, 2008] and remeasuring field plots to assess errors requires additional resources. Additionally, existing data sets of vegetation plots, such as Forest Inventory and Analysis in the U.S., may neither provide the necessary sampling density, nor contain plots along the transects that ICESAT and DESDynI data are, or will be, collected in. For all of these reasons, there remains a need to identify efficient ways to collect ground truth data across large spatial extents for quantifying vegetation structure and biomass.

[8] Thoughtful sampling designs can improve the efficiency of field data collection and results of subsequent remote sensing analyses using field sampled data. Regression models are typically used to relate field data to remotely sensed data and then make broad-scale predictions. The accuracy of modeled vegetation structure and biomass can be improved if field data are collected across the entire range of variability in the population. If random sampling is used to select locations for field data collection, it is likely that points at the edge of the data distribution will be missed, especially when only a small fraction of the entire population can be sampled [*Thompson*, 2002]. This is problematic, because points at the edge of the data distribution can be highly influential on regression model fit, and model predictions made beyond the range over which the data were collected can often lead to unreliable or unreasonable results [*Chatterjee et al.*, 2000].

[9] Stratified sampling includes data points at the edge of the data distribution by design, and this ensures that the regression models are not extrapolating beyond the range of the field data and tends to reduce regression model prediction errors. Stratified samples have been used in prior LiDAR studies, with strata being defined based on management history [*Lim et al.*, 2003], or forest age and site index [*Næsset*, 1997b, 2002]. Such stratification surpasses random sampling designs, but assumes that ancillary information is available, and uses forest attributes likely to affect vegetation structure as the basis for stratification, rather than the actual data. To our knowledge, only one study has used the actual LiDAR data to stratify their field sample [*van Aardt et al.*, 2006], and no study has systematically compared a stratified sample based on LiDAR data with a random sample. Such a comparison would be valuable given the need for effective sampling designs for field data, and the opportunities that broad-scale LiDAR data provides for stratification, and ultimately for vegetation structure and biomass assessments.

[10] Thus, in this study, we had two goals, 1) to estimate forest vegetation structure and biomass across broad areas using LiDAR data as a predictor, and 2) to compare a random field sampling design to a stratified sampling design using LiDAR data as prior information.

2. Methods

2.1. Study Area

[11] We conducted our analysis in forested, public lands of Oconto County in northeastern Wisconsin. This area covers nearly 53,600 ha and landforms are primarily glacial in origin [*Martin*, 1965]. Historically, forests in these landscapes were dominated by jack pine (*Pinus banksiana*) and red pine (*Pinus resinosa*) on light, sandy upland soils and white pine (*Pinus strobus*) on sandy loams. Mixed forests occurred on heavier soils with white pine, hemlock (*Tsuga canadensis*), balsam fir (*Abies balsamea*), white spruce (*Picea glauca*), sugar maple (*Acer saccharum*), basswood (*Tilia americana*), yellow birch (*Betula alleghaniensis*), beech (*Fagus sylvatica*), American elm (*Ulmus americana*), red oak (*Quercus rubra*), and ironwood (*Ostrya virginiana*) [*Curtis*, 1959]. Logging was extensive and peaked in the late nineteenth century [*Flader*, 1983]. Following logging, farming was promoted and attempted in many areas, but many farms ultimately failed and forests are again extensive in this region although managed harvesting continues [*Gough*, 1997]. All tree species still occur, but the present composition of tree species is more homogenous than it once was, and broadleaf species are now more common and needle-leaved species less common than they were historically [*Schulte et al.*, 2007].

[12] Public lands are extensive in Oconto County and there are 45,100 ha of forest in the Chequamegon-Nicolet National Forest and 8,500 ha in county forests. We restricted our field sampling to these areas to facilitate property access. Land ownership boundaries for the Chequamegon-Nicolet National Forest and Oconto County Forests were provided by the WI DNR [*Wisconsin Department of Natural Resources*, 2008].

[13] An existing land cover classification based on Landsat imagery [*Wisconsin Department of Natural Resources*, 1998] was used to split potential sampling locations into deciduous and coniferous forest and to exclude sampling in other land cover types (i.e., agriculture and urban). We grouped mixed forests with deciduous forests because there appeared to be spatial inconsistencies in where mixed forest was mapped and there was not a substantial amount of mixed forest on the landscape. In the field, most coniferous forest pixels were truly coniferous and deciduous forest pixels contained a mixture of both coniferous and deciduous tree species.

2.2. LiDAR Data Collection

[14] LiDAR data were collected using a Leica ALS50 flown in leaf-off conditions during May of 2005 with an altitude of about 2,000 m (6,500 ft) and flight speed of 240 km/h LiDAR pulse frequency was 34,700 Hz and the beam footprint was 68.9 cm (2.26 feet). These LiDAR data contained 1–3 returns and the density of all returns was 0.4 returns/m^2. The horizontal accuracy of pulses was estimated to be 0.5 m. The ground-truthed vertical accuracy was estimated to be 15 cm RMSE.

2.3. LiDAR Data Processing Methods

[15] The LiDAR data were first used to construct a digital elevation model of the ground surface with 5 m resolution. Second, we extracted all LiDAR pulses that fell in public lands and classified them according to forest type, coniferous or deciduous using the land cover classification. All of these pulses were considered to have reflected off either vegetation or the ground. The height above ground was calculated by subtracting the ground elevation from each pulse elevation. Pulses heights less than 1 m and greater than 50 m were considered to be either ground or 'noise' and were excluded from the analysis. The remaining pulses were aggregated to 30-m pixels (the same resolution as the land cover data) and the mean and standard deviation of pulse heights were calculated for each pixel (μ_{lidar}, σ_{lidar}, respectively). Other LiDAR summary metrics, such as LiDAR height quantiles [*Hopkinson et al.*, 2006; *Næsset*, 1997a; Hawbaker et al., submitted manuscript, 2009] and the height above median energy for waveform LiDAR [*Anderson et al.*, 2006; *Drake et al.*, 2002], have been used to estimate vegetation structure and biomass. Exploratory analysis of our data found the correlation between mean and median LiDAR height was 0.99. Additionally, previous research in similar forests types in southern Wisconsin demonstrated that the mean and standard deviation of LiDAR height are highly correlated with LiDAR height quantiles and explain a similar amount of variability in vegetation structure present on the landscape (Hawbaker et al., submitted manuscript, 2009).

2.4. Sampling Designs for Field Data

[16] Each forested pixel with aggregated mean and standard deviation of LiDAR height values were potential sampling locations. We compiled two sampling data sets for comparison. The first was a random sample stratified only by forest type. The second was a stratified sample that used LiDAR data to define additional strata within forest types. In the first, random sample design, we randomly selected 30 pixels classified as coniferous forest and 60 pixels classified as deciduous forest for sampling locations. We selected a greater number of pixels in deciduous forest because the landscape was primarily deciduous forest and we expected greater variability in tree species composition and vegetation structure there. Some of the plots fell on private land and were not accessible. Thus, our final random sample sizes consisted of 28 plots in coniferous forest and 53 plots in deciduous forest.

[17] Our second design used a stratified sampling approach and we used the aggregated LiDAR height measurements as prior information to stratify potential field sampling locations across our study area. For each forest type, potential sampling locations were stratified into 10 strata according to the mean LiDAR height and then within each stratum, an additional stratification into 3 strata according to the standard deviation of LiDAR height was made (Figure 1). This produced 30 stratifications total and within each stratum, we randomly selected one coniferous forest and two deciduous forest locations. This resulted in a total of 30 coniferous forest plots and 60 deciduous forest plots for sampling,

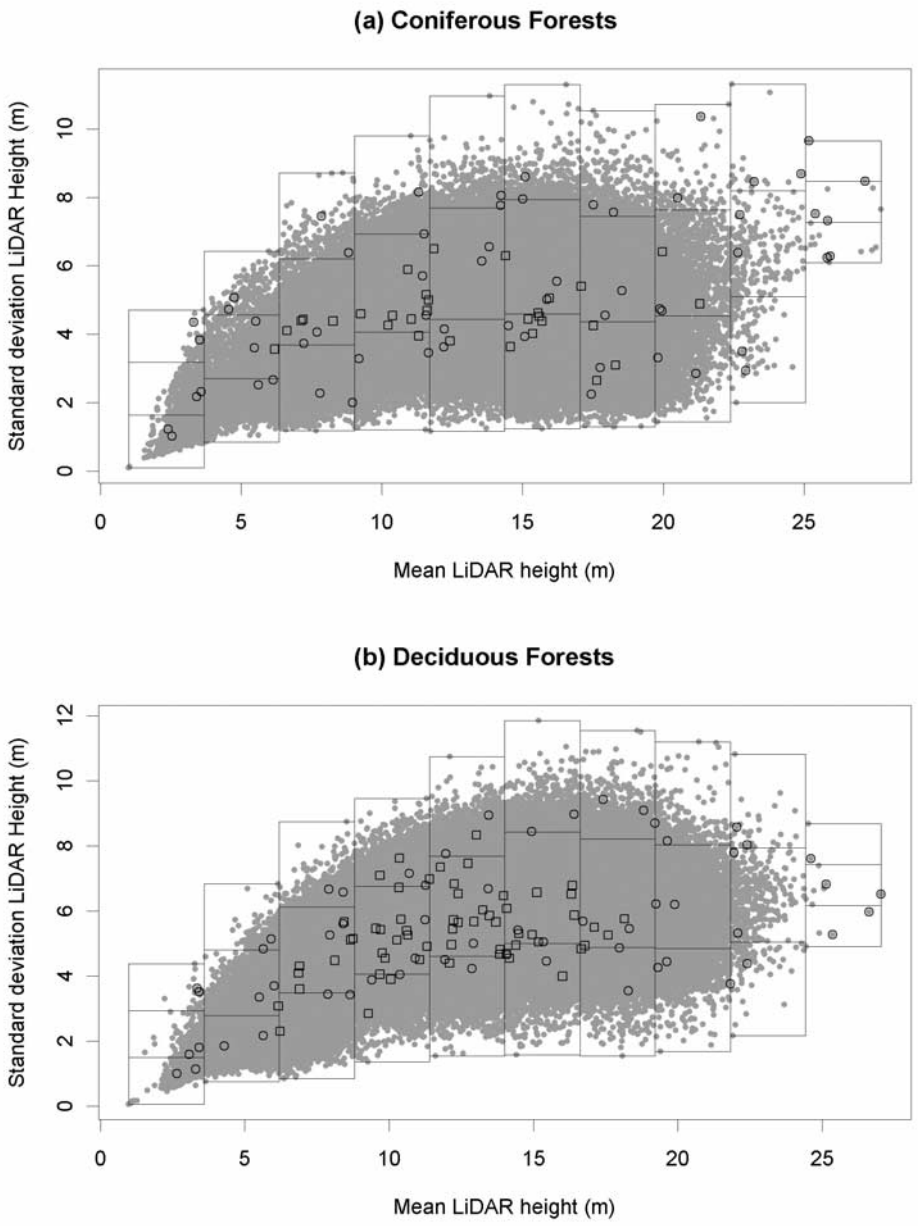

Figure 1. Example of deciduous forest sampling locations selected from all potential sites (gray solid dots) using a completely random sample (open squares) and a hierarchical-stratified sample (open circles) for (a) coniferous forests and (b) deciduous forests. Data were stratified first by the mean of LiDAR pulse height (x axis) and then by the standard deviation of LiDAR pulse height (y axis). Black lines show the breaks among hierarchical strata.

out of which 27 coniferous forest plots and 52 deciduous forest plots were accessible and measured.

[18] We conducted exploratory data analysis comparing the distribution of mean LiDAR height and standard deviation of LiDAR height for the entire population, to distributions from the random and stratified samples. Both sampling designs estimated the mean of the population well. However, the stratified sampling included a greater range of variability in mean and standard deviation of LiDAR heights than the random sampling (Figure 2). The motivation for the stratified sampling design; was not necessarily to capture the exact distribution of the population but to include more data points in the tips and the tails of the data distribution. We anticipated that models constructed from the stratified sample would perform better than models constructed from the random sample.

2.5. Field Data Collection

[19] We used handheld global positioning systems (GPS) to navigate to field sites until the GPS reported the location was within 20 m, then maintained our heading and walked exactly 20 paces to the final plot location. This procedure introduced a level of randomness in establishing the exact plot location, and ensured that plot locations would not be

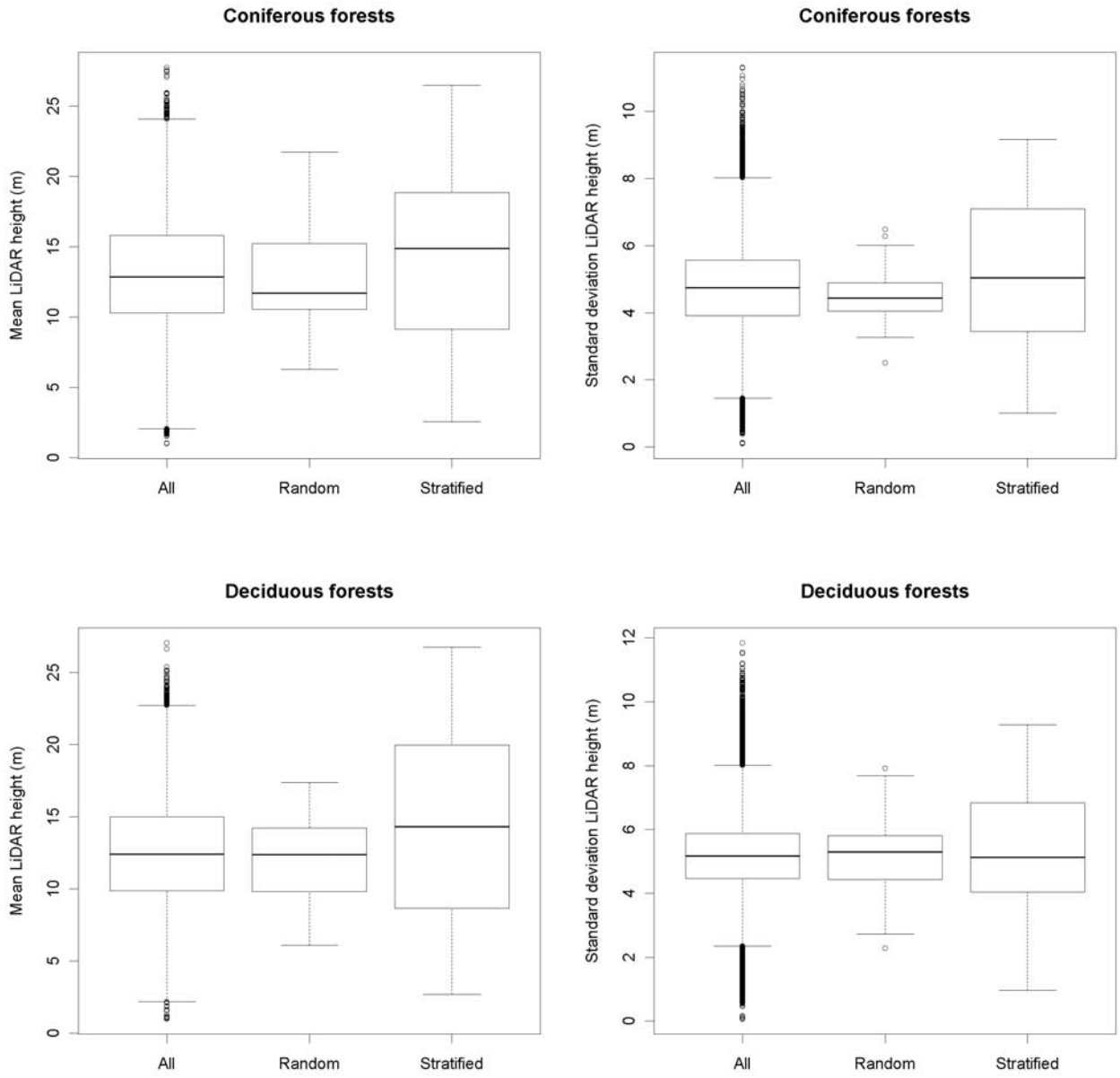

Figure 2. Boxplots showing the median, quartiles, maximum, minimum, and range of values for predictor variables, mean and standard deviation of LiDAR height, for all the locations that could have been sampled, locations in the random sample, and locations in the stratified samples for both coniferous and deciduous forests.

biased by field technicians reluctant to walk through dense understory vegetation. Once the plot center was established, we recorded the actual plot location with a Trimble ProXH GPS, which was later postprocessed to submeter accuracy.

[20] At each plot location, we recorded species and measured the diameters of all trees with diameter at breast height (DBH) $\geq$ 12.7 cm that were within 17 m of the plot center. Total tree height was measured for a subset of trees selected using a 2.3 m^2/ha (10 ft^2/acre) basal-area factor prism. On average, there were 45 trees in each plot, and heights were typically measured for 11 of them. Height measurements from these trees were used to build regression models to predict total height for the remaining trees. DBH was used to predict tree height and both DBH and tree height were log transformed [*Avery and Burkhart*, 2002]. We accounted for plot-level differences in the relationship between tree height and DBH by allowing the intercept and slope to vary among plots using a linear mixed-effects model [*Gelman and Hill*, 2007; *Pinherio and Bates*, 2002]. The root-mean square error (RMSE) for the natural log of tree height in the resulting model was 0.15. Using the measured DBH, we calculated total tree biomass using species-specific allometric equations [*Jenkins et al.*, 2003]. Finally, individual tree measurements were summarized to the plot level (Table 1). These plot-level summaries included mean DBH (cm), mean tree height (m), basal area (m^2/ha), and biomass (megagrams/ha or Mg/ha).

Table 1. Summaries of Field Vegetation Data

	Coniferous						Deciduous					
	Random		Stratified		Combined		Random		Stratified		Combined	
	Mean	SD	Mean	SD	Mean	SD	Mean	SD	Mean	SD	Mean	SD
DBH (cm)	23.93	4.20	27.80	8.30	25.83	6.77	22.75	4.94	25.84	8.02	24.28	6.79
ln(1 + BA) [ln(1 + m^2/ha)]	3.33	0.45	3.16	0.96	3.25	0.74	2.95	0.63	2.90	0.84	2.92	0.74
Mean tree height[a] (m)	18.85	3.46	20.61	6.31	19.71	5.09	3.01	0.15	3.06	0.33	3.03	0.25
Biomass (Mg/ha)	149.50	95.51	165.74	117.96	157.47	134.57	129.26	82.97	139.97	88.17	106.43	85.34

[a]Mean tree height values for deciduous forests were natural log + 1 transformed.

2.6. Regression Analysis

[21] Our first goal was to make countywide predictions of vegetation structure and biomass. To accomplish this goal, we used regression models to relate the plot-level summaries of field tree measurements (mean DBH, total basal area, mean tree height, total tree biomass) to plot-level LiDAR height summaries; (mean lidar height, μ_{lidar}, and standard deviation of lidar height, σ_{lidar}; Figure 3). For countywide predictions, we constructed regression models using all sampling locations for a given forest type. Including all field sample locations ensured that models were well specified and captured the trend in the data. In our models, we initially included μ_{lidar} and σ_{lidar} as predictor variables. However, predictors were removed if they were not significant (p values > 0.05).

[22] There were slight, nonlinear trends in the relationships between mean DBH and μ_{lidar} and σ_{lidar} and total basal area and μ_{lidar} for coniferous forests (Figure 3). We tested various data transformations to improve linear model fits and found that natural log transformations improved models of basal area for both forest types and mean tree height for deciduous forests. More complicated, nonlinear models may have explained the data better; however, our sample sizes were small and there were few degrees of

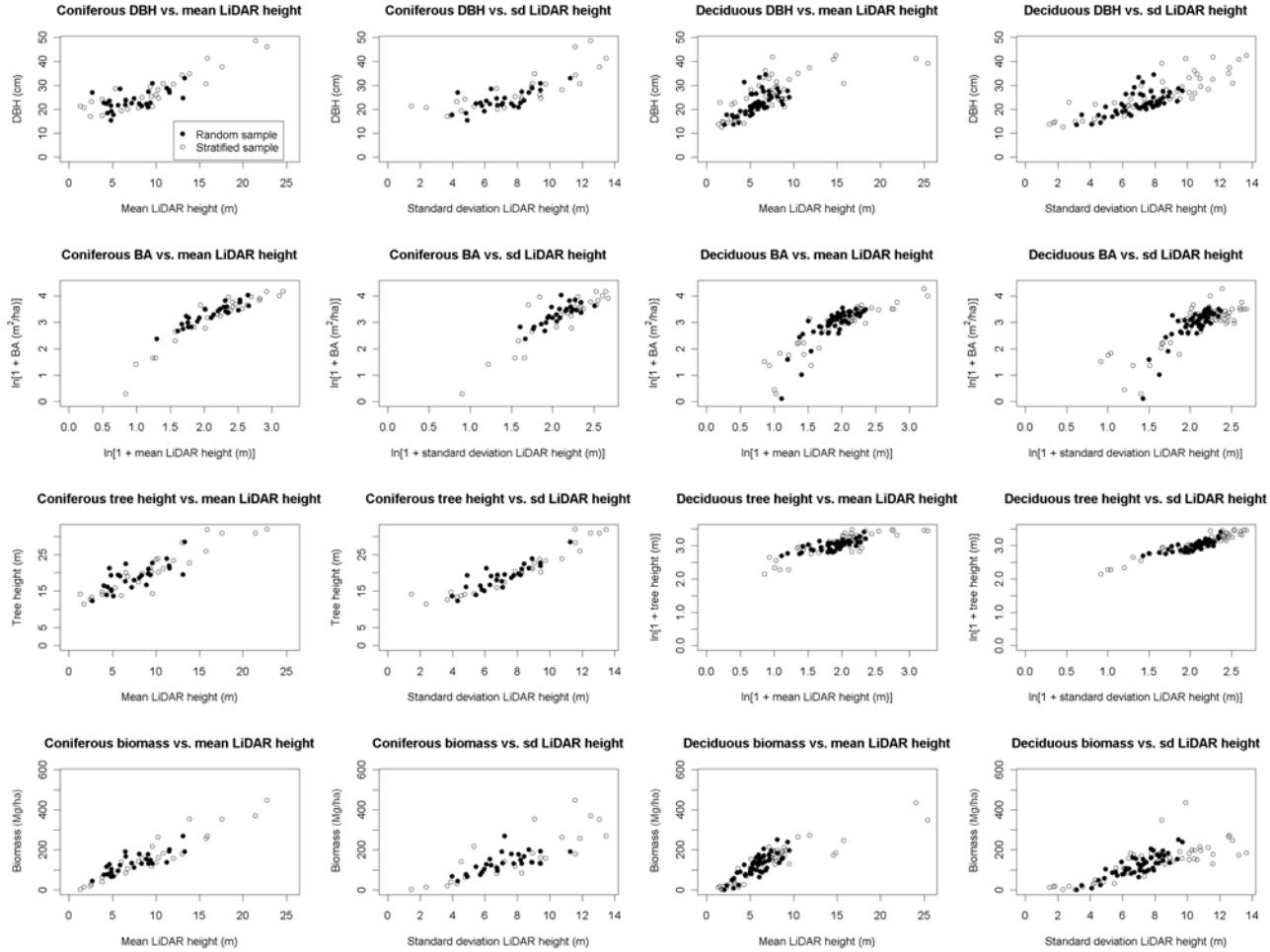

Figure 3. Scatterplots of field measured mean diameter at breast height (DBH), basal area (BA), mean tree height, and total biomass against mean and standard deviation in LiDAR heights for coniferous and deciduous forests.

Table 2. Model Results by Forest Type Using All Sampled Locations[a]

Model Data	Model Form	R^2	$RMSE_{model}$	Units
Coniferous	$DBH = f(\mu_{lidar} + \sigma_{lidar})$	0.71	3.60	cm
Deciduous	$DBH = f(\mu_{lidar} + \sigma_{lidar})$	0.73	3.47	cm
Coniferous	$\ln(BA + 1) = f[\ln(\mu_{lidar} + 1)]$	0.81	0.32	$\ln(1 + m^2/ha)$
Deciduous	$\ln(BA + 1) = f[\ln(\mu_{lidar} + 1)]$	0.65	0.43	$\ln(1 + m^2/ha)$
Coniferous	mean tree height $= f(\mu_{lidar} + \sigma_{lidar})$	0.88	1.78	$\ln(1 + m)$
Deciduous	$\ln(\text{mean tree height} + 1) = f[\ln(\sigma_{lidar} + 1) + \ln(\sigma_{lidar} + 1)]$	0.88	0.09	$\ln(1 + m)$
Coniferous	biomass $= f(\mu_{lidar})$	0.75	45.55	Mg/ha
Deciduous	biomass $= f(\mu_{lidar} + \sigma_{lidar})$	0.71	39.32	Mg/ha

[a]Here μ_{lidar} is the mean of LiDAR pulse heights and σ_{lidar} is the standard deviation of LiDAR pulse heights.

freedom available to fit nonlinear models well. Therefore, we continued the analysis with linear regression models. In spite of the slight nonlinear trends, the scatterplots show that the randomly sampled points did not capture the nonlinear patterns in the data as well as the stratified sample.

[23] Our second goal was to evaluate the two sampling designs and their influence on prediction errors for vegetation structure and biomass. To accomplish this goal, we used the predictor variables selected in the countywide models but estimated regression coefficient values using only the data from each sample design. By using the previously established countywide model form, each sampling design could be evaluated as to how well it captured the trends. This resulted in four models for each tree measurement corresponding to the two sample designs and two forest types (coniferous random, coniferous stratified, deciduous random, and deciduous stratified).

[24] For each model, we calculated the root mean squared error (RMSE) using the model predictions and observations from the data set used to construct the model, referred to as $RMSE_{model}$. Then, we validated models by making predictions for the other sample design and calculated the RMSE from its predictions and observations, referred to as $RMSE_{validate}$. Thus, models built with the stratified sample were validated with the random sample and vice versa. We expected that models built using the stratified sample would have $RMSE_{model}$ values similar to $RMSE_{validate}$. Because the random samples may not have included values at the edges of the data distribution, which are more difficult to predict, we expected $RMSE_{model}$ for models built using the random sample would be less than $RMSE_{validate}$.

3. Results

3.1. Countywide Model Results

[25] Regression models generated using all the sample locations for each forest type explained a large proportion of the variability in the data (65 to 88%; Table 2). Models for mean tree height had the best fits, followed by coniferous basal area, total biomass and then mean DBH. In almost all models, both the mean and standard deviation of LiDAR height (μ_{lidar} and σ_{lidar}) were significant predictor variables (p value ≥ 0.05). Mean LiDAR height (μ_{lidar}) was the only significant predictor in models of basal area.

[26] Regression models for coniferous forests tended to explain more variability than models for deciduous forests, except for mean tree height where model R^2 values were equal between forest types. RMS errors were low for mean DBH, basal area, and mean tree height and ranged from 3 to 15% of the mean observed values. However, RMS errors for total biomass were larger, at 29% of the mean observed value for both coniferous and deciduous forests (Table 2).

3.2. Influence of Sample Design on Model Predictions

[27] Overall, regression models constructed using either sample design explained vegetation structure and biomass well (Table 3). As was the case for the models constructed with the full sample, mean DBH models explained the least amount of variability. However, there were key differences

Table 3. Model Results and Errors for Individual Sampling Designs[a]

Model Data	Validation Data	Model Form	R^2	$RMSE_{model}$	$RMSE_{validate}$	Units
CS	CR	$DBH = f(\mu_{lidar} + \sigma_{lidar})$	0.76	3.56	3.91	cm
CR	CS	$DBH = f(\mu_{lidar} + \sigma_{lidar})$	0.54	3.20	5.17	cm
DS	DR	$DBH = f(\mu_{lidar} + \sigma_{lidar})$	0.84	3.57	3.69	cm
DR	DS	$DBH = f(\mu_{lidar} + \sigma_{lidar})$	0.41	3.56	3.72	cm
CS	CR	$\ln(BA + 1) = f[\ln(\mu_{lidar} + 1)]$	0.90	0.30	0.36	m^2/ha
CR	CS	$\ln(BA + 1) = f[\ln(\mu_{lidar} + 1)]$	0.84	0.17	0.44	m^2/ha
DS	DR	$\ln(BA + 1) = f[\ln(\mu_{lidar} + 1)]$	0.79	0.38	0.41	$\ln(1 + m^2/ha)$
DR	DS	$\ln(BA + 1) = f[\ln(\mu_{lidar} + 1)]$	0.69	0.35	0.49	$\ln(1 + m^2/ha)$
CS	CR	mean tree height $= f(\mu_{lidar} + \sigma_{lidar})$	0.91	1.91	1.77	m
CR	CS	mean tree height $= f(\mu_{lidar} + \sigma_{lidar})$	0.73	1.75	1.95	m
DS	DR	$\ln(\text{mean tree height} + 1) = f[\ln(\mu_{lidar} + 1) + \ln(\sigma_{lidar} + 1)]$	0.90	0.10	0.09	$\ln(1 + m)$
DR	DS	$\ln(\text{mean tree height} + 1) = f[\ln(\mu_{lidar} + 1) + \ln(\sigma_{lidar} + 1)]$	0.68	0.08	0.11	$\ln(1 + m)$
CS	CR	biomass $= f(\mu_{lidar} + \sigma_{lidar})$	0.89	37.66	34.63	Mg/ha
CR	CS	biomass $= f(\mu_{lidar} + \sigma_{lidar})$	0.66	29.24	48.70	Mg/ha
DS	DR	biomass $= f(\mu_{lidar} + \sigma_{lidar})$	0.84	34.54	31.40	Mg/ha
DR	DS	biomass $= f(\mu_{lidar} + \sigma_{lidar})$	0.74	27.44	47.61	Mg/ha

[a]CS, coniferous stratified; CR, coniferous random; DS, deciduous stratified; DR, deciduous random; μ_{lidar}, mean lidar pulse height; σ_{lidar}, the standard deviation in lidar pulse height.

between of the random and the LiDAR-stratified sampling design.

[28] Comparing the two sample designs, R^2 values were generally lower for the random sample models, but R^2 is dependent on the range of sample values [*Gelman and Hill*, 2007] and can be expected to be higher for a stratified sample, since a greater data range is sampled. As one would also expect, regression models constructed using the random sample generally had $RMSE_{model}$ values lower than those for the stratified sample. This was not surprising since the random sample focuses on the center of the data distribution, which is easier to predict. The difference in $RMSE_{model}$ between the two sample designs was large for coniferous forests and ranged between 32 and 39%, except for models of mean tree height where the difference in $RMSE_{model}$ was 12% (Table 3). Differences in $RMSE_{model}$ between sampling designs in deciduous forests were less pronounced and were between 5 and 9%, except for biomass where the stratified sampling design produced models with $RMSE_{model}$ 31% less than models using data from the random sampling design (Table 3).

[29] Generating predictions for one sample design with models built using the other sample design demonstrated the strengths and weaknesses of the two sample designs. The random sample models performed poorly when predicting values for the stratified sample ($RMSE_{validate}$). This was especially evident for models of basal area, mean DBH, and biomass in coniferous forests where $RMSE_{validate}$ for the random sample models were up to 113%, 100% and 76% greater than $RMSE_{model}$ respectively (Table 3). These results indicated that the random sample models were not able to provide good predictions beyond the narrow range of data used to build them.

[30] In contrast to the random models, there was little increase in error when stratified sample models were used to predict values for the random sample. The differences between $RMSE_{model}$ and $RMSE_{validate}$ for the stratified models were overall fairly small (Table 3). In most cases the difference between $RMSE_{model}$ and $RMSE_{validate}$ was less than 16%, except for the stratified model of coniferous forest biomass where the difference was 36%. These results demonstrated that the stratified sample models were able to predict the random sample data nearly as well as they could predict the stratified sample data used to fit them. In other words, the stratified sample models predicted well at both the center and at the edges of the distribution.

4. Discussion

[31] Our results showed that accurate quantification of the spatial variability in forest vegetation structure and biomass across broad spatial extents is possible using low-density LiDAR data originally collected for terrain mapping. Our findings confirmed previous studies that demonstrated that consistent methods of processing and summarizing LiDAR can be used across different vegetation types to estimate vegetation structure and biomass, although the exact shape of the relationship may vary [*Hopkinson et al.*, 2006; *Lefsky et al.*, 2005b; *Lim et al.*, 2003]. Consequently, airborne LiDAR sensors provide a valuable tool for broad-scale characterization of vegetation structure while requiring minimal field data collection.

[32] Mean LiDAR height was included in all models of vegetation structure and biomass and was the only significant variable for basal area and coniferous forest biomass. However, standard deviation of LiDAR height explained additional variability in vegetation structure and was also included in most other models. Our choice of mean and standard deviation as LiDAR height metrics was somewhat arbitrary and other metrics, such as height quantiles, have proven to have greater explanatory power [*Næsset*, 2002, 2004]. However, previous research in similar forests types in southern Wisconsin demonstrated that mean LiDAR height explained nearly as much variability in forest structure as other height metrics (Hawbaker et al., submitted manuscript, 2009). Although other LiDAR metrics may have explained slightly more variability in the vegetation structure and biomass, we believe the mean and standard deviation explained a sufficient amount of variability in the data to compare the effectiveness of different sampling designs, a primary goal of our analysis. Our results demonstrated that the stratified sampling design almost always produced lower model errors and we believe the results would hold true regardless of which metrics were used to summarize the LiDAR height data. In any case, both mean and standard deviation of LiDAR height and additional variables [*Næsset*, 2002] can be easily calculated from LiDAR pulse data that are summarized to grids and allow for efficient processing of the large volumes of data generated by LiDAR missions.

[33] The comparison of the two sampling design highlighted the advantages of stratified sampling designs and strongly suggests that LiDAR or other remotely sensed data could be used to optimize sampling designs. The LiDAR stratification ensured that the entire data range of the predictor variables was sampled on the ground, and this resulted in better predictions by LiDAR-derived regression models. Well-planned sampling designs can greatly improve predictive results for models based on remotely sensed data. In contrast, random sampling did not capture the full range of data. Thus, when regression models based on randomly sampled data are extrapolated across broad scales, one of the major assumptions of regression is violated; that predictions are made within the same range of data used to build the model [*Chatterjee et al.*, 2000]. Sometimes, existing data are available and can provide valuable information to help determine where to locate collection of field data. Previous studies using LiDAR data for mapping forest structure have relied on management history [*Lim et al.*, 2003], as well as forest age and site index [*Næsset*, 1997a, 2002]; however, these data are not available in many regions. Stratifying data prior to analysis is common practice for many remote sensing applications [*Carlotto*, 1998; *McRoberts et al.*, 2002; *Potapov et al.*, 2008]. However; the use of LiDAR data to delineate stratum prior to collection of field data is another alternative, but appears to be rarely used (except see *van Aardt et al.* [2006]). Our findings suggest that using LiDAR or other remotely sensed data to guide sampling designs will result in efficient collection of field data and produce improved modeled results over simple random sampling. Additionally, such sampling strategies are a practical necessity given that making model predictions based from a random sample will almost inva-

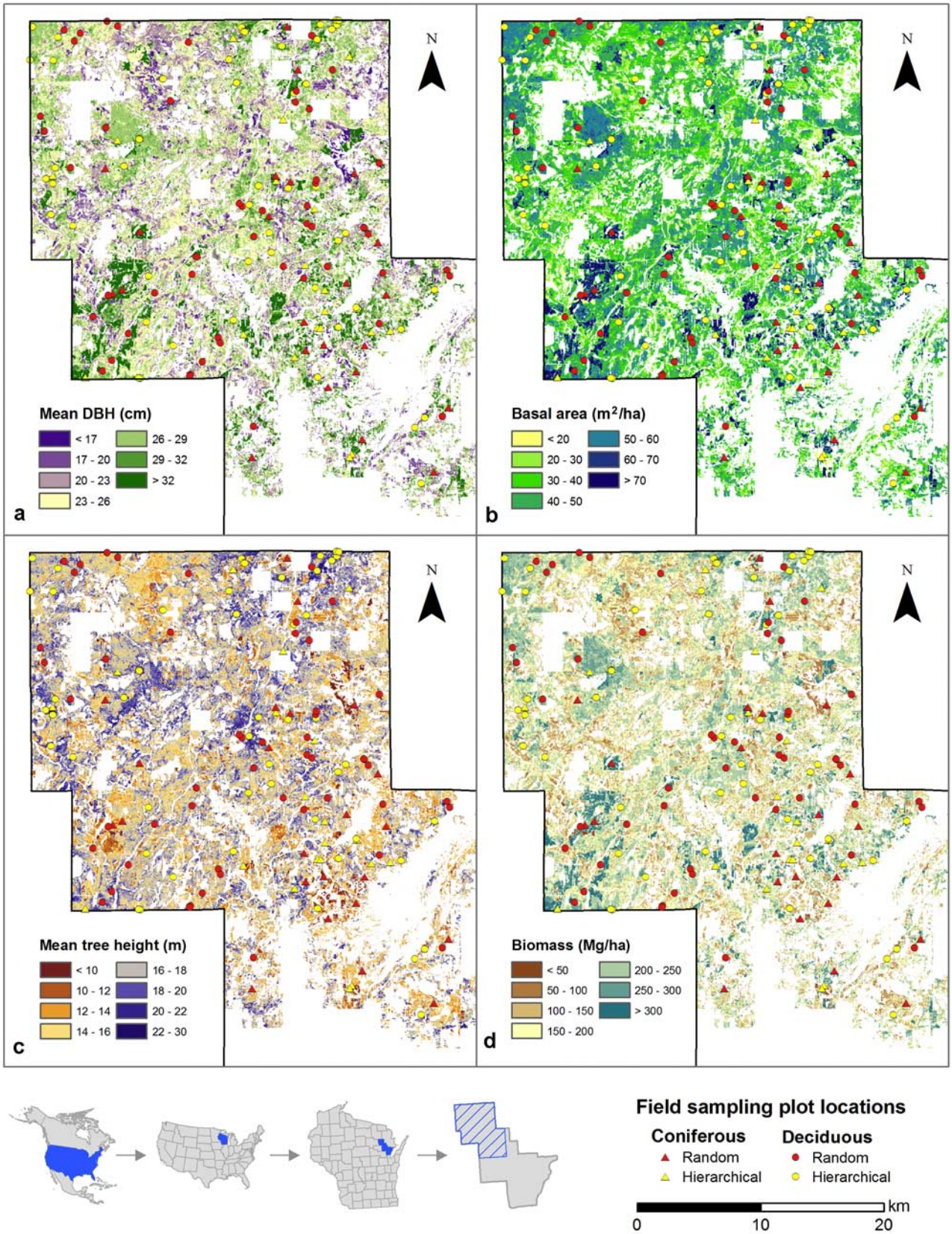

Figure 4. Mapped (a) mean diameter at breast height (DBH; cm), (b) basal area (m^3/ha), (c) mean tree height (m), and (d) biomass (Mg/ha) for Oconto County, Wisconsin, United States. White areas did not have LiDAR data, were not forest, or were privately owned and not accessible.

riably result in the need to extrapolate past the range of the observed predictors.

[34] The magnitude of prediction errors could potentially be reduced by increasing sample sizes. However, prediction errors were generally greater for models constructed from a random sample of field data. In order to match the accuracy of a stratified design, more data would need to be collected from a substantially greater number of plots in a random sampling design. Thus, thoughtful sampling designs can result in higher predictive accuracy than random sampling designs with the added benefit of requiring less effort for field data collection.

[35] Our LiDAR-based maps of vegetation structure and biomass provided a detailed assessment for a fairly large study area (53,600 ha), and such broad-scale assessments are key in order to translate LiDAR data into information relevant for forest managers. Our LiDAR maps were derived from low-density LiDAR data. As such, the prediction error rates are probably similar to what could be expected from a spaceborne mission, like DESDynI. The question is if the prediction errors are acceptable for management purposes as well. Our prediction errors were similar to those found for tree heights and lower than those found for basal area in previous LiDAR-based studies in similar forest types [*Lim et al.*, 2003; Hawbaker et al., submitted manuscript, 2009]. However, our prediction errors are still about 2 to 5 times larger than measurement errors typical for forestry field inventories [*Avery and Burkhart*, 2002], but the key is that our predictions are wall-to-wall, whereas forestry field inventories provide data for sampling points only.

[36] The richer information that a wall-to-wall map of vegetation structure (Figure 4) and biomass provides counterbalances the operationally large prediction errors. Commonly, forest inventory sample plots are aggregated at the forest stand level, and intrastand level heterogeneity is not mapped. The LiDAR maps of forest attributes provide much more spatial detail, which can be as important for management decisions as lower confidence intervals. Additionally, the LiDAR maps can be aggregated to forest stands or other spatial management units, and such aggregation will reduce the overall error because pixel-level errors will cancel out [*Næsset*, 2002]. Thus, even though error rates may be high for any individual location, our estimates of vegetation structure are likely to be accurate when viewed across broad spatial extents. Spaceborne LiDAR systems, such as the proposed DESDynI sensor, thus have the potential to provide key information on vegetation structure and biomass for management purposes, but LiDAR data should not replace but rather be used in conjunction with field data.

[37] Perhaps most importantly, LiDAR data can provide information for the vast areas of our planet for which we have very little information, either because they are privately owned and gaining access is often difficult, or because they are so remote that field visits are rare. There will be new opportunities for quantifying patterns of vegetation structure and biomass across broad spatial scales with the release of the Landsat data archive [*U.S. Geological Survey*, 2008] and the pending availability of data from new active remote sensors, such as DESDynI. The resolutions at which these sensors collect data (~30 m) are amenable to sampling field data. Assessments of vegetation structure and biomass often rely on data collected both through remote sensing and fieldwork. Regardless of the sensor used (LiDAR, Landsat, DESDynI, etc.), our study highlights the great potential of remotely sensed data for vegetation assessments, especially when they are well integrated with the design of field data collection efforts.

[38] **Acknowledgments.** LiDAR data were provided by Ayers Associates, Inc. and Oconto County; their willingness to share data made this project possible. All field plots were located on lands in the Chequamegon-Nicolet National Forest and Oconto County Forest. Wisconsin Department of Natural Resources graciously provided funding to collect field data for this project. Dan Olson and Kristin Rhode were responsible for all field data collection. We are grateful for comments provided by three anonymous reviewers; they helped to improve the scope and quality of this manuscript.

References

Anderson, J., et al. (2006), The use of waveform lidar to measure northern temperate mixed conifer and deciduous forest structure in New Hampshire, *Remote Sens. Environ.*, *105*(3), 248–261.

Avery, T. E., and H. E. Burkhart (2002), *Forest Measurements*, 5th ed., McGraw-Hill, Boston, Mass.

Bauer, M. E., et al. (1994), Satellite inventory of Minnesota forest resources, *Photogramm. Eng. Remote Sens.*, *60*(3), 287–298.

Bergen, K. M., et al. (2007), Multi-dimensional vegetation structure in modeling avian habitat, *Ecol. Inform.*, *2*(1), 9–22.

Brandtberg, T., et al. (2003), Detection and analysis of individual leaf-off tree crowns in small footprint, high sampling density lidar data from the eastern deciduous forest in North America, *Remote Sens. Environ.*, *85*(3), 290–303.

Carlotto, M. J. (1998), Spectral shape classification of landsat thematic mapper imagery, *Photogramm. Eng. Remote Sens.*, *64*(9), 905–913.

Chatterjee, S., et al. (2000), *Regression Analysis by Example*, 3rd ed., John Wiley, New York.

Cohen, W. B., and T. A. Spies (1992), Estimating structural attributes of douglas-fir western hemlock forest stands from Landsat and SPOT imagery, *Remote Sens. Environ.*, *41*(1), 1–17.

Cramer, W., et al. (2001), Global response of terrestrial ecosystem structure and function to CO2 and climate change: Results from six dynamic global vegetation models, *Global Change Biol.*, *7*(4), 357–373.

Curtis, J. T. (1959), *The Vegetation of Wisconsin*, Univ. of Wis. Press, Madison.

Donnellan, A., et al. (2008), Deformation, ecosystem structure, and dynamics of ice (DESDynI), in *Proceedings of IEEE Aerospace Conference*, IEEE Press, Piscataway, N. J.

Drake, J. B., et al. (2002), Estimation of tropical forest structural characteristics, using large-footprint lidar, *Remote Sens. Environ.*, *79*(2–3), 305–319.

Fassnacht, K. S., et al. (1997), Estimating the leaf area index of North Central Wisconsin forests using the Landsat Thematic Mapper, *Remote Sens. Environ.*, *61*(2), 229–245.

Flader, S. L. (1983), *The Great Lakes Forest: An Environmental and Social History*, Univ. of Minn. Press, Minneapolis.

Gelman, A., and J. Hill (2007), *Data Analysis Using Regression and Multilevel/Hierarchical Models*, Cambridge Univ. Press, Cambridge, U. K.

Gobakken, T., and E. Næsset (2008), Assessing effects of laser point density, ground sampling intensity, and field sample plot size on biophysical stand properties derived from airborne laser scanner data, *Can. J. For. Res.*, *38*, 1095–1109.

Goetz, S., et al. (2007), Laser remote sensing of canopy habitat heterogeneity as a predictor of bird species richness in an eastern temperate forest, USA, *Remote Sens. Environ.*, *108*(3), 254–263.

Gough, R. J. (1997), *Farming the Cutover: A Social History of Northern Wisconsin, 1900–1940*, Univ. Press of Kansas, Lawrence.

Gower, S. T., et al. (1999), Direct and indirect estimation of leaf area index, f(APAR), and net primary production of terrestrial ecosystems, *Remote Sens. Environ.*, *70*(1), 29–51.

Harding, D. J., and C. C. Carabajal (2005), ICESat waveform measurements of within-footprint topographic relief and vegetation vertical structure, *Geophys. Res. Lett.*, *32*, L21S10, doi:10.1029/2005GL023471.

Hopkinson, C., et al. (2006), Towards a universal lidar canopy height indicator, *Can. J. Rem. Sens.*, *32*(2), 139–152.

Hyde, P., et al. (2006), Mapping forest structure for wildlife habitat analysis using multi-sensor (LiDAR, SAR/InSAR, ETM plus, Quickbird) synergy, *Remote Sens. Environ.*, *102*(1–2), 63–73.

Hyyppä, J., et al. (2001), A segmentation-based method to retrieve stem volume estimates from 3-D tree height models produced by laser scanners, *IEEE Trans. Geosci. Remote Sens.*, *39*(5), 969–975.

Jakubauskas, M. E., and K. P. Price (1997), Empirical relationships between structural and spectral factors of Yellowstone lodgepole pine forests, *Photogramm. Eng. Remote Sens.*, *63*(12), 1375–1381.

Jenkins, J. C., et al. (2003), National-scale biomass estimators for United States tree species, *For. Sci.*, *49*(1), 12–35.

Leckie, D., et al. (2003), Combined high-density lidar and multispectral imagery for individual tree crown analysis, *Can. J. Rem. Sens.*, *29*(5), 633–649.

Lefsky, M. A., et al. (2002), Lidar remote sensing for ecosystem studies, *BioScience*, *52*(1), 19–30.

Lefsky, M. A., et al. (2005a), Estimates of forest canopy height and aboveground biomass using ICESat, *Geophys. Res. Lett.*, *32*, L22S02, doi:10.1029/2005GL023971.

Lefsky, M. A., et al. (2005b), Geographic variability in lidar predictions of forest stand structure in the Pacific Northwest, *Remote Sens. Environ.*, *95*(4), 532–548.

Lim, K., et al. (2003), Lidar remote sensing of biophysical properties of tolerant northern hardwood forests, *Can. J. Rem. Sens.*, *29*(5), 658–678.

MacArthur, R. H., and J. W. MacArthur (1969), On bird species diversity, *Ecology*, *42*, 594–598.

Maclean, G. A., and W. B. Krabill (1986), Gross-merchantable timber volume estimation using an airborne lidar system, *Can. J. Rem. Sens.*, *12*(1), 7–18.

Magnusson, M., et al. (2007), Effects on estimation accuracy of forest variables using different pulse density of laser data, *For. Sci.*, *53*(6), 619–626.

Martin, L. (1965), *The Physical Geography of Wisconsin*, Univ. of Wis. Press, Madison.

McRoberts, R. E., et al. (2002), Stratified estimation of forest area using satellite imagery, inventory data, and the k-Nearest Neighbors technique, *Remote Sens. Environ.*, *82*(2–3), 457–468.

Næsset, E. (1997a), Estimating timber volume of forest stands using airborne laser scanner data, *Remote Sens. Environ.*, *61*(2), 246–253.

Næsset, E. (1997b), Determination of mean tree height of forest stands using airborne laser scanner data, *ISPRS J. Photogramm. Remote Sens.*, *52*(2), 49–56.

Næsset, E. (2002), Predicting forest stand characteristics with airborne scanning laser using a practical two-stage procedure and field data, *Remote Sens. Environ.*, *80*(1), 88–99.

Næsset, E. (2004), Practical large-scale forest stand inventory using a small-footprint airborne scanning laser, *Scand. J. For. Res.*, *19*(2), 164–179.

Næsset, E., et al. (2004), Laser scanning of forest resources: The Nordic experience, *Scand. J. For. Res.*, *19*(6), 482–499.

Nelson, R., et al. (1984), Determining forest canopy characteristics using airborne laser data, *Remote Sens. Environ.*, *15*(3), 201–212.

Nelson, R., et al. (1988), Estimating forest biomass and volume using airborne laser data, *Remote Sens. Environ.*, *24*(2), 247–267.

Nilsson, M. (1996), Estimation of tree weights and stand volume using an airborne lidar system, *Remote Sens. Environ.*, *56*(1), 1–7.

Pinherio, J. C., and D. M. Bates (2002), *Mixed-Effects Models in S and S-PLUS*, Springer, New York.

Potapov, P., et al. (2008), Combining MODIS and Landsat imagery to estimate and map boreal forest cover loss, *Remote Sens. Environ.*, *112*(9), 3708–3719.

Schulte, L. A., et al. (2007), Homogenization of northern U. S. Great Lakes forests due to land use, *Landscape Ecol.*, *22*, 1089–1103.

Thompson, S. K. (2002), *Sampling*, 2nd ed., John Wiley, New York.

U.S. Geological Survey (2008), Imagery for everyone, technical announcement, Reston, Va.

van Aardt, J. A. N., et al. (2006), Forest volume and biomass estimation using small-footprint lidar-distributional parameters on a per-segment basis, *For. Sci.*, *52*(6), 636–649.

Vierling, K. T., et al. (2008), Lidar: Shedding new light on habitat characterization and modeling, *Front. Ecol. Environ.*, *6*(2), 90–98.

Westfall, J. A. (2008), Differences in computed individual-tree volumes caused by differences in field measurements, *North. J. Appl. For.*, *25*(4), 195–201.

Wisconsin Department of Natural Resources (1998), Wisconsin land cover grid, Madison.

Wisconsin Department of Natural Resources (2008), WI DNR GIS data holdings, Madison. (Available at ftp://dnrftp01.wi.gov/geodata/)

Wolter, P. T., et al. (1995), Improved forest classification in the northern Lake-States using multitemporal Landsat imagery, *Photogramm. Eng. Remote Sens.*, *61*(9), 1129–1143.

Zheng, D. L., et al. (2004), Estimating aboveground biomass using Landsat 7 ETM+ data across a managed landscape in northern Wisconsin, USA, *Remote Sens. Environ.*, *93*(3), 402–411.

K. Contrucci, Ayers Associates, Inc., 1802 Pankratz Street, Madison, WI 53704, USA. (contruccik@ayresassociates.com)

T. Gobakken, Department of Ecology and Natural Resource Management, Norwegian University of Life Sciences, P.O. Box 5003, NO-1432 Ås, Norway. (terje.gobakken@umb.no)

T. J. Hawbaker, A. A. Lesak, and V. C. Radeloff, Department of Forest and Wildlife Ecology, University of Wisconsin-Madison, 1630 Linden Drive, Madison, WI 53706, USA. (tjhawbaker@gmail.com; lesak@wisc.edu; radeloff@wisc.edu)

N. S. Keuler, Department of Statistics, University of Wisconsin-Madison, 1300 University Avenue, Madison, WI 53706, USA. (nskeuler@wisc.edu)